Regular Article

PHYSICAL CHEMISTRY RESEARCH
Published by the
Iranian Chemical Society
www.physchemres.org
info@physchemres.org

Phys. Chem. Res., Vol. 8, No. 3, 529-542, September 2020
DOI: 10.22036/pcr.2020.224934.1749

First-order Nonlinear Optical Response of $C_2B_{n-2}H_{n-1}X$ (n = 14-17; X = H, Li, Na, K, F, Cl, Br) Carboranes: Insights from DFT and TD-DFT Calculations

M. Yousefizadeh, E. Shakerzadeh* and M. Bamdad

Chemistry Department, Faculty of Science, Shahid Chamran University of Ahvaz, Ahvaz, Iran

(Received 29 March 2020, Accepted 24 May 2020)

Density functional theory (DFT) and time-dependent density functional theory (TD-DFT) calculations were employed to investigate the electronic and nonlinear optical properties of some substituted $C_2B_{n-2}H_n$ (n = 14-17) carboranes. Li, Na, K, F, Cl, Br are used as substituents. The carboranes substituted with alkali metal show considerably large first hyperpolarizability values than those of un-substituted ones. The nonlinear optical (NLO) response of the halogen substituted systems is slightly enhanced. The well-known two-level model theory is investigated through TD-DFT approach to understand the origin of NLO response. This study indicates that alkali-metal substituted carboranes may be appropriate for NLO applications.

Keywords: Carborane, Nonlinear optical (NLO), First hyperpolarizability, DFT calculations

INTTRODUCTION

Nonlinear optical (NLO) materials have been received incessant interest owing to their various applications in optoelectronic modulators [1-6]. The design and synthesis of NLO materials have been considered owing to their potential applications in optical telecommunication and photonic usages [7-11]. The total magnitude of the first static hyperpolarizability (β_0) is known as the first order nonlinear optical response coefficient, which can be considered as one of the microscopic parameters of macroscopic NLO materials. Various efficient strategies have been proposed to induce the static first hyperpolarizability (β_0) [12]. The diffuse excess electron molecular systems are in great interest of computational chemists. In this regard, the literature is notably rich in theoretical investigations about alkali metals-molecular systems with high nonlinear optical response because of the diffuse excess electrons of alkali metals [13-17]. Li and coworkers [18-20] presented new ideas to produce the diffuse excess electron through the interaction between the alkali atom and the polar molecules in electrides to decrease the excitation energy and improve the first hyperpolarizability of systems.

Carboranes as an important class of boron-containing rigid structures have potential applications in medicinal drug design [21]. The stability trend of $C_nB_{n-2}H_n$ (n = 5-12) carboranes with increasing size has been studied by Schleyer and co-workers using *ab initio* calculations [22]. They are polyhedral boron hydride clusters, which each of them has one or more B(H) vertices replaced by C(H) units. Two cage-carbon-atom arrangements of carboranes include the carbon-atoms-adjacent (CAd) isomers and the carbon-atoms-apart (CAp) isomers. In the former, the cage carbon atoms occupy adjacent positions, while the cage carbon atoms are separated by at least one boron atom in the latter. Since the discovery of dicarba-closo-dodecaboranes (12), they have been used in various applications such as catalysis [23-26], materials design [27,28] and medicine [29]. These cluster compounds show extraordinary thermal stability and unusual chemical reactivity. These properties cause a broad range of their applications such as encompassing organic synthesis, drug design, polymers, cancer therapy and metal-

---

*Corresponding author. E-mail: e.shakerzadeh@scu.ac.ir

organic frameworks [30]. That is why, the carboranes and metallacarboranes are attractive compounds for researchers [31,32]. The structure, synthesis, reactivity, and applications of these clusters have been reported by several groups [33-37]. Herein, it is of interest to investigate the impact of Li, Na, K, F, Cl, NH_2 and NO_2 substitutions in $C_2B_{n-2}H_n$ (n = 14-17) carboranes. The NLO response of these systems were studied and compared with each other.

Computational Details

The molecular geometries without symmetry constraints were optimized at BH and HLYP/6-31+G(d) level of theory. The nature of the stationary points is checked by frequency analysis at the same computational level and no imaginary frequency is observed for the considered structures. All the systems were considered as neutral in charge and having multiplicity M = 1 ($M = 2S + 1$, S = total spin).

The HOMO-LUMO energy gap (HLG) was calculated according to the highest occupied molecular orbital (ε_H) and the lowest unoccupied molecular orbital (ε_L) energies as follows:

$$HLG = \varepsilon_L - \varepsilon_H \tag{1}$$

Also, the material's work function ($\Phi = E_{\text{inf}} - E_f$) denotes the minimum energy required for removing an electron from the Fermi level (E_f) to a point far enough not to be affected by the material. Therefore, the electrostatic potential at infinity (E_{inf}) is assumed to be zero. It is well-known that emitted electron current densities (j) in the vacuum are exponentially related to the wok function as follows:

$$j = AT^2 \exp\left(\frac{-\Phi}{kT}\right) \tag{2}$$

$$\Phi = E_{\text{inf}} - E_f = -\frac{\varepsilon_L + \varepsilon_H}{2} \tag{3}$$

in which A stands for the Richardson constant. It is noteworthy that tuning the work function of materials has an important role in electronic industry. Modulating the work function of material can remarkably control the performance of electronic device performance such as the field emission properties. The change in energy gap (%ΔHLG) or work function (%ΔΦ) were computed as follows:

$$\%\Delta W = \frac{[W_{C_2B_{n-2}H_{n-1}X} - W_{C_2B_{n-2}H_n}]}{W_{C_2B_{n-2}H_n}} \times 100 \tag{4}$$

where $W_{C_2B_{n-2}H_n}$ and $W_{C_2B_{n-2}H_{n-1}X}$ stand for the energy gap or work function values of the un-substituted and substituted carboranes, respectively. These parameters exhibit the electronic sensitivity of the considered carboranes toward alkali metals or halogen substitution.

The first-order hyperpolarizability has been computed at the ground state optimized geometry. The energy of a molecule can be expressed through Taylor series expansion in the presence of an external homogeneous electric field (F) as follows:

$$E = E^{(0)} - \sum_i \mu_i^{(0)} F_i - \frac{1}{2!}\sum_i \sum_j \alpha_{ij} F_i F_j - \frac{1}{3!}\sum_i \sum_j \sum_k \beta_{ijk} F_i F_j F_k - \frac{1}{4!}\sum_i \sum_j \sum_k \sum_l \gamma_{ijkl} F_i F_j F_k F_l \tag{5}$$

and thereby the corresponding induced electric dipole moment of the molecule becomes:

$$\mu_i = \mu_i^{(0)} + \sum_j \alpha_{ij} F_j + \frac{1}{2!}\sum_j \sum_k \beta_{ijk} F_j F_k + \frac{1}{3!}\sum_j \sum_k \sum_l \gamma_{ijkl} F_j F_k F_l. \tag{6}$$

where $\mu^{(0)}$ denotes the permanent ground state dipole moment, and α, β and γ the coefficients are known as polarizability, first- and second-hyperpolarizability, respectively. The total magnitude of the first static hyperpolarizability (β_0) was calculated accordingly:

$$\beta_0 = [(\beta_{xxx} + \beta_{xyy} + \beta_{xzz})^2 + (\beta_{yyy} + \beta_{yxx} + \beta_{yzz})^2 + (\beta_{zzz} + \beta_{zxx} + \beta_{zyy})^2]^{1/2} \tag{7}$$

The β_{xxx}, β_{yxy}, β_{xyy},… components were assessed at BHandHLYP/6-311++G(d) level. Meanwhile, the origin of the NLO response of the investigated species has been

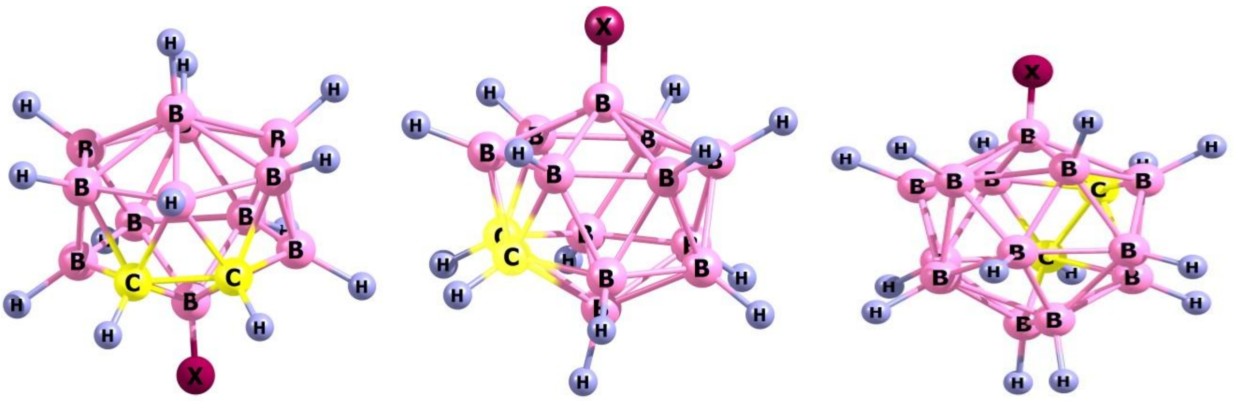

$C_2B_{12}H_{14}$(I) $C_2B_{12}H_{14}$(II) $C_2B_{13}H_{15}$

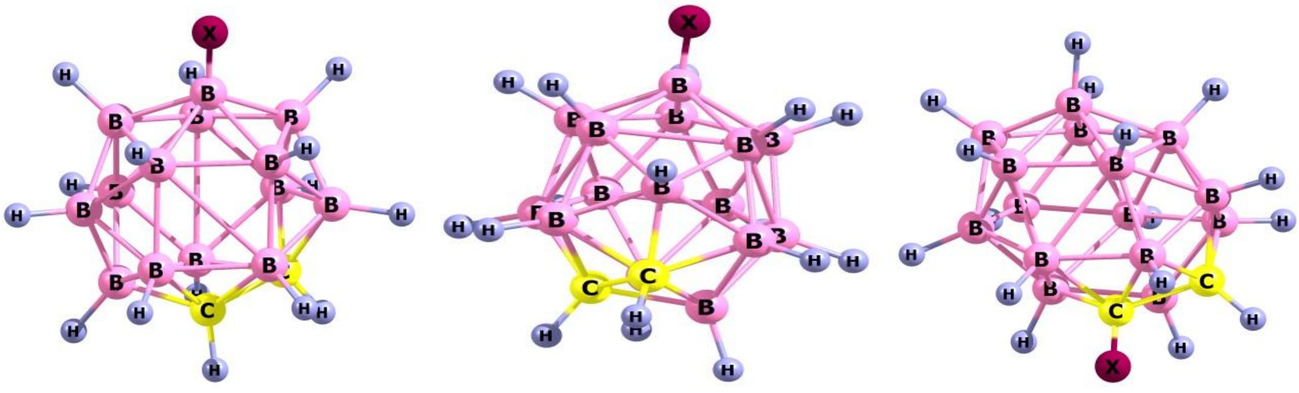

$C_2B_{14}H_{16}$(II) $C_2B_{15}H_{17}$(I) $C_2B_{15}H_{17}$(II)

Fig. 1. The schematic structures of the studied compounds.

invoked through the two-level model [38]. The time dependent density functional (TD-DFT) calculations at BHand HLYP/6-311++G(d) level were applied to calculate the electronic properties of each system for about 30 lower-lying excited states. Based on the two-level model, the first static hyperpolarizability expresses as follows:

$$\beta_0 \propto \frac{\Delta\mu f_0}{\Delta E^3} \tag{8}$$

where ΔE, f_0 and Δμ are the transition energy, oscillator strength, and the difference of the dipole moment between the ground state and the crucial excited state, respectively. The crucial excited state has the greatest oscillator strength among the excited ones. All calculations are carried out using Gaussian 09 software.

RESULTS AND DISCUSSION

The most stable carbon-atoms-adjacent (CAd) positional isomers of $C_2B_{n-2}H_n$ (n = 14-17) were selected from previous reports [48-51]. The schematic structures are exhibited in Fig. 1. The hydrogen atom, connected to the boron or carbon atom at the vertices, is substituted by

Table 1. The Frontier Molecular Orbital Energy (ε_H and ε_L), HOMO-LUMO Gap (HLG) and Work Function as Well as their Percentage of Variation ($\%\Delta\text{HLG}$, $\%\Delta\Phi$), and the NBO Charge on Substituent (q_x)

Molecules	HOMO (eV)	LUMO (eV)	HLG (eV)	ΔHLG (%)	Φ (eV)	%ΔΦ	q_x	β_0
2,3-$C_2B_{12}H_{14}$	-9.24	-1.01	8.22	-	5.13	-	-	19.28
$C_2B_{12}H_{13}Li$	-6.75	-1.31	5.45	-33.74	4.03	-21.44	0.90	2898.48
$C_2B_{12}H_{13}Na$	-6.30	-1.47	4.84	-41.17	3.89	-24.27	0.84	7306.29
$C_2B_{12}H_{13}K$	-5.63	-1.38	4.25	-48.37	3.51	-31.68	0.93	10174.15
$C_2B_{12}H_{13}F$	-9.40	-1.22	8.19	-0.41	5.31	3.51	-0.50	112.47
$C_2B_{12}H_{13}Cl$	-9.39	-1.25	8.14	-1.00	5.32	3.70	-0.10	125.30
$C_2B_{12}H_{13}Br$	-9.29	-1.27	8.02	-2.43	5.28	2.92	-0.20	73.86
$C_2B_{12}H_{13}Li(II)$	-5.91	-0.93	4.98	-39.46	3.42	-33.33	0.86	4322.68
$C_2B_{12}H_{13}Na(II)$	-5.49	-1.06	4.43	-46.17	3.28	-36.16	0.78	9635.45
$C_2B_{12}H_{13}K(II)$	-4.72	-1.03	3.69	-55.15	2.88	-43.96	0.88	17042.50
$C_2B_{12}H_{13}F(II)$	-9.40	-1.18	8.21	-0.13	5.29	3.12	-0.52	136.59
$C_2B_{12}H_{13}Cl(II)$	-9.39	-1.25	8.14	-1.05	5.32	3.70	-0.14	147.24
$C_2B_{12}H_{13}Br(II)$	-8.88	-1.28	7.60	-7.54	5.08	-0.97	-0.31	53.90
$C_2B_{13}H_{15}$	-8.83	-2.16	6.67	-	5.50	-	-	27.40
$C_2B_{13}H_{14}Li$	-6.28	-1.44	4.83	-27.47	3.86	-29.75	0.89	3691.37
$C_2B_{13}H_{14}Na$	-5.87	-1.53	4.34	-34.88	3.70	-32.67	0.83	9325.13
$C_2B_{13}H_{14}K$	-5.97	-1.43	4.54	-31.83	3.70	-32.67	0.98	2483.26
$C_2B_{13}H_{14}F$	-9.03	-2.36	6.67	0.03	5.70	3.64	-0.51	120.28
$C_2B_{13}H_{14}Cl$	-9.01	-2.40	6.61	-0.81	5.71	3.82	-0.12	125.54
$C_2B_{13}H_{14}Br$	-8.88	-2.46	6.46	-3.14	5.67	3.18	-0.22	64.15
$C_2B_{14}H_{16}$	-9.40	-1.01	8.39	-	5.21	-	-	51.35
$C_2B_{14}H_{15}Li$	-5.64	-0.92	4.73	-43.65	3.28	-37.04	0.87	5931.38
$C_2B_{14}H_{15}Na$	-5.29	-1.10	4.18	-50.14	3.20	-36.68	0.79	13548.12
$C_2B_{14}H_{15}K$	-5.02	1.21	3.81	-54.60	1.91	-63.44	0.96	10334.44
$C_2B_{14}H_{15}F$	-9.41	1.21	8.20	-2.28	4.10	-21.31	-0.51	188.52
$C_2B_{14}H_{15}Cl$	-8.99	-1.26	7.73	-7.79	5.13	-1.63	-0.13	252.77

Table 1. Continued

$C_2B_{14}H_{15}Br$	-8.46	-1.29	7.17	-14.54	4.88	-6.43	-0.21	159.85
$C_2B_{15}H_{17}$	-9.15	-0.52	8.62	-	4.84	-	-	55.59
$C_2B_{15}H_{16}Li$	-5.61	-0.76	4.85	-43.71	3.19	-28.34	0.84	6439.82
$C_2B_{15}H_{16}Na$	-5.21	-0.87	4.34	-49.66	3.04	-30.82	0.75	13198.22
$C_2B_{15}H_{16}K$	-4.51	-0.91	3.60	-58.27	2.71	-36.47	0.84	25883.39
$C_2B_{15}H_{16}F$	-9.32	-0.61	8.71	0.98	4.97	2.14	-0.51	236.55
$C_2B_{15}H_{16}Cl$	-9.02	-0.65	8.37	-2.92	4.84	-0.09	-0.13	308.72
$C_2B_{15}H_{16}Br$	-8.48	-0.66	7.81	-9.40	4.57	-4.62	-0.26	213.23
$C_2B_{15}H_{16}Li$(II)	-8.33	-1.47	6.86	-20.44	4.90	1.03	0.93	563.42
$C_2B_{15}H_{16}Na$(II)	-7.92	-1.89	6.03	-30.09	4.91	1.11	0.91	1283.62
$C_2B_{15}H_{16}K$(II)	-7.50	-1.60	5.90	-31.53	4.55	-4.97	0.98	890.79
$C_2B_{15}H_{16}F$(II)	-9.37	-0.60	8.76	1.64	4.99	2.48	-0.33	79.20
$C_2B_{15}H_{16}Cl$(II)	-9.31	-0.64	8.66	0.48	4.98	2.31	-0.11	38.58
$C_2B_{15}H_{16}Br$(II)	-9.28	-0.98	8.30	-3.71	5.13	4.97	0.09	202.73

different groups in order to evaluate the impact of substitution on the electro-optical features. The substituted structures are achieved by replacing the hydrogen atom at the vertices by Li, Na, K, F, Cl, or Br group. In the case of $C_2B_{12}H_{14}$, two boron atoms locate at two vertices. One of them is in hexagonal ring composed of boron atoms, and the other one is in the hexagonal ring with both boron and carbon atoms. The $C_2B_{13}H_{15}$ and $C_2B_{14}H_{16}$ structures have one boron atom at the vertex. Indeed, the $C_2B_{15}H_{17}$ structure has two vertices. One vertex has boron atom and the other one has carbon atom.

The frontier molecular orbital energies (HOMO (ε_H) and LUMO (ε_L)) and the HOMO-LUMO gap (HLG) of the considered systems are listed in Table 1. Accordingly, the HLG values in substituted molecules are less than un-substituted cases. For instance, the substitutions of alkali metals in $C_2B_{12}H_{14}$ (I), $C_2B_{12}H_{14}$ (II), $C_2B_{13}H_{15}$, $C_2B_{14}H_{16}$, $C_2B_{15}H_{17}$ (I) and $C_2B_{15}H_{17}$ (II) systems cause to decrease the HLG values by about 48.37%, 55.15%, 31.83%, 54.6%, 58.27% and 31.53%, respectively. This may due to this fact that the alkali metals substitutions strongly influence the HOMO energy level; whereas the LUMO energy level has no obvious change. Furthermore, such remarkable HLG changes are not observed by F, Cl and Br substituents. The HLGs are nearly unchanged for these substituted molecules. Table 1 summarizes the obtained work function values of the considered structures. The results demonstrate that the substitution of alkali metals in carboranes remarkably decreases the work functions; whereas these values nearly remain constant by halogen substitution. Therefore, the considered alkali metals substituted carborane exhibit a considerable emitted electron current density. The Natural bond orbital (NBO) analysis is also performed using Gaussian NBO Version 3.1 [39] and the NBO charges are collected in Table 1. It is obvious that the alkali-metal substituents have a positive charge, whereas halogens have a negative charge. Therefore, it seems that the alkali-metal groups are able to push an electron while the halogens are

Table 2. The TD-DFT Parameters, Major Electronic Transitions and the First Hyperpolarizability (β_0) Values of the Considered Systems

Molecules	β_0 (a.u.)	ΔE (eV)	f_0	Δμ	Major contributions
$C_2B_{12}H_{14}$(I)					
$C_2B_{12}H_{14}$	19.28	6.09	0.04	0.24	HOMO→L+1 (79%)
$C_2B_{12}H_{13}Li$	2898.48	3.34	0.13	1.57	HOMO→LUMO (96%)
$C_2B_{12}H_{13}Na$	7306.29	3.19	0.32	4.04	HOMO→LUMO (93%)
$C_2B_{12}H_{13}K$	10174.15	2.74	0.21	3.13	HOMO→LUMO (87%)
$C_2B_{12}H_{14}$ (II)					
$C_2B_{12}H_{13}Li$	4322.68	2.93	0.14	1.89	HOMO→LUMO (96%)
$C_2B_{12}H_{13}Na$	9635.45	2.88	0.34	4.80	HOMO→LUMO (99%)
$C_2B_{12}H_{13}K$	17042.50	2.28	0.22	3.96	HOMO→LUMO (96%)
$C_2B_{13}H_{15}$					
$C_2B_{13}H_{15}$	27.40	8.20	0.03	0.17	H-2→L+6 (19%), HOMO→L+7 (11%)
$C_2B_{13}H_{14}Li$	3691.37	3.05	0.11	1.43	HOMO→L+1 (92%)
$C_2B_{13}H_{14}Na$	9325.13	2.96	0.26	3.53	HOMO→L+1 (67%)
$C_2B_{13}H_{14}K$	2483.26	4.55	0.06	0.51	HOMO→L+3 (58%),
$C_2B_{14}H_{16}$					
$C_2B_{14}H_{16}$	51.35	7.04	0.11	0.65	H-4→L (21%), H-2→L+2(23%)
$C_2B_{14}H_{15}Li$	5931.38	2.71	0.16	2.37	HOMO→LUMO (96%)
$C_2B_{14}H_{15}Na$	13548.12	2.61	0.38	5.92	HOMO→LUMO (92%)
$C_2B_{14}H_{15}K$	10334.44	2.38	0.13	2.17	HOMO→LUMO (96%)
$C_2B_{15}H_{17}$(I)					
$C_2B_{15}H_{17}$	55.59	7.93	0.07	0.36	H-7→L+3(53%)
$C_2B_{15}H_{16}Li$	6439.82	2.82	0.16	2.36	HOMO→LUMO (95%)
$C_2B_{15}H_{16}Na$	13198.22	2.82	0.40	5.79	HOMO→LUMO (99%)
$C_2B_{15}H_{16}K$	25883.39	2.24	0.30	5.40	HOMO→LUMO (96%)
$C_2B_{15}H_{17}$(II)					
$C_2B_{15}H_{16}Li$	563.42	6.88	0.05	0.32	HOMO→L+4 (46%),
$C_2B_{15}H_{16}Na$	1283.62	4.20	0.06	0.58	HOMO→LUMO (93%)
$C_2B_{15}H_{16}K$	890.79	4.34	0.03	0.30	HOMO→LUMO (92%)

unable.

The first hyperpolarizability of the considered systems are calculated using Eq. (7). The values of β_0 are summarized in Table 2. It can be seen that β_0 values are noticeably large for alkali-metal substituted carboranes, but these values are slightly increased for halogen substituted ones with respect to un-substituted systems. This observation reveals that the alkali-metal is a better choice for increasing the β_0 value. Results show that the alkali-metal substituted carboranes have larger first hyperpolarizability values than other carborane derivatives. The potassium substituted $C_2B_{12}H_{14}$ (I), $C_2B_{12}H_{14}$ (II) and $C_2B_{15}H_{17}$ (I) have the greatest β_0 value. The β_0 values of $C_2B_{12}H_{13}K$ (I), $C_2B_{12}H_{13}K$ (II) and $C_2B_{15}H_{16}K$ (I) are 10174.15, 17042.50 and 25883.39 a.u., respectively. For better description, the trend of β_0 values variation is presented in Fig. 2.

As can be seen in Eq. (8), $\Delta\mu$ values influence on values of the first hyperpolarizability. Therefore it can be concluded that positive charges of substituent lead to increase in $\Delta\mu$ and thereby NLO response remarkably is increased. However, having negative charges of substituents with the ability to pull an electron leads to a slight change of the NLO responses. Based on the Eq. (5), the β_0 value is considerably dependent on the values of ΔE. These mentioned parameters are also computed and listed in Table 2. The TD-DFT calculations are employed to attain the major effects of the crucial excited states. As seen in this table, the values of ΔE and f_0 for alkali-metal substituted carboranes are greater and smaller, respectively, than other carboranes. A larger NLO response can be obtained from a larger transition moment, larger oscillator strength, and lower transition energy. Based on Eq. (8), β_0 is considerably dependent to the inverse value of ΔE. These structures have the least amount of ΔE. In $C_2B_{13}H_{15}$, $C_2B_{14}H_{16}$ and $C_2B_{15}H_{17}$ (II), alkali-metal substituted carboranes with Na atom have the greatest β_0 value. The β_0 values of $C_2B_{13}H_{14}Na$, $C_2B_{14}H_{15}Na$ and $C_2B_{15}H_{16}Na$ (II) are 9325.13, 13548.12 and 1283.62 a.u, respectively. The ΔE values of $C_2B_{13}H_{14}Na$ and $C_2B_{15}H_{16}Na$ (II) are the smallest, and the f_0 and $\Delta\mu$ have the highest values compared with other alkali-metal derivatives. In $C_2B_{14}H_{16}$, the ΔE values of alkali-metal derivatives do not differ significantly, while $C_2B_{14}H_{15}Na$ has the highest value of f_0 and $\Delta\mu$.

The TD-DFT results illustrate that the main excited transformations of most systems are the transitions of HOMO to LUMO, HOMO to LUMO+1. These transitions in alkali-metal substituted carboranes have different effects. For instance, the transition from HOMO to LUMO and from HOMO to LUMO+1 generate electron spectra, also the transitions from HOMO to LUMO generate charge transfers from the carborane cage to alkali-metal. The electron transition effort is proportional to the energy gap between LUMO and HOMO. As a result, the electron transition effort for alkali-metal substituted carboranes is much lower and the corresponding first hyperpolarizability is much larger. The frontier molecular orbitals of alkali-metal substituted systems in their ground state and crucial excited state are shown in Fig. 3. The electron transition among the frontier molecular orbitals produces charge transfers. These transfers occur from vertex B atoms to the center of carborane. For alkali-metal substituted carboranes, the HOMO electron clouds, which are polarized by the carborane cage, move toward the outer layer of the alkali metal atom but the LUMO electron cloud remains in the local area of the alkali-metal and its connected B atom. Large transitions cause a large cloud distribution difference between HOMO and LUMO. This difference leads to a large charge transfer range from the carborane cage to the alkali metal. This large value makes easier the leave of the electron on the outer orbital of the alkali-metal. The ionized alkali atom forms a cation and some free electron anions, making the alkali metal positively charged. It can be implied that positive charges on alkali-metal become larger.

The infrared photodissociation has been known as a prominent technique to characterize the novel species in gas phases. Thus, the vibrational spectra of the studied structures are also depicted in Fig. 4. A somewhat simple vibrational spectra are observed. The subsunts have a remarkable impact on the vibrational spectra. Also, the optoelectronic properties such as UV-Vis absorption spectra may provide valuable insights. Thus, the time dependent density functional method (TD-DFT) has been used to predict the optical absorption spectra of the alkali-metals substituted carboranes for about 30 lower lying excited states. These spectra are displayed in 5. The absorption

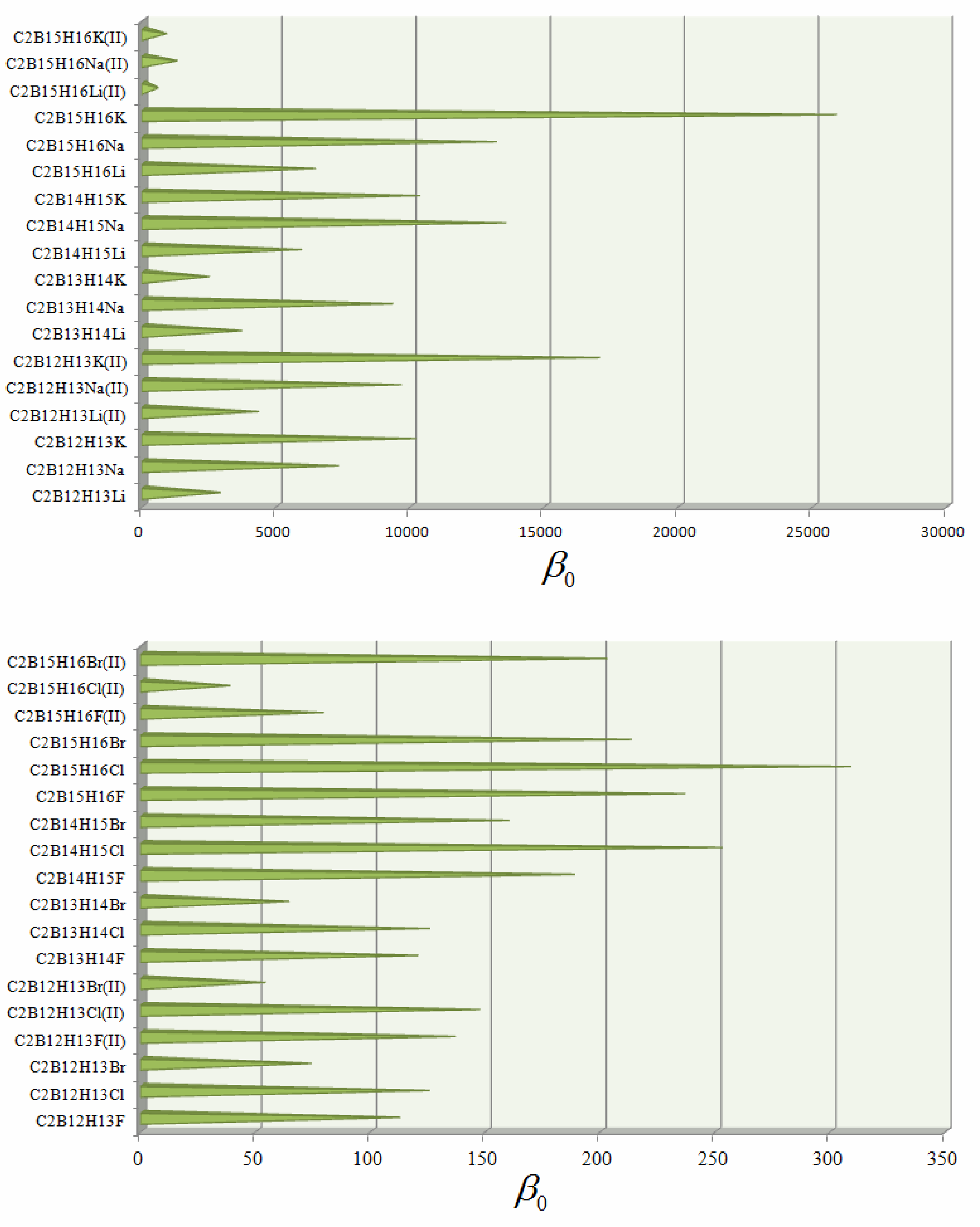

Fig. 2. The trend of β_0 values variation.

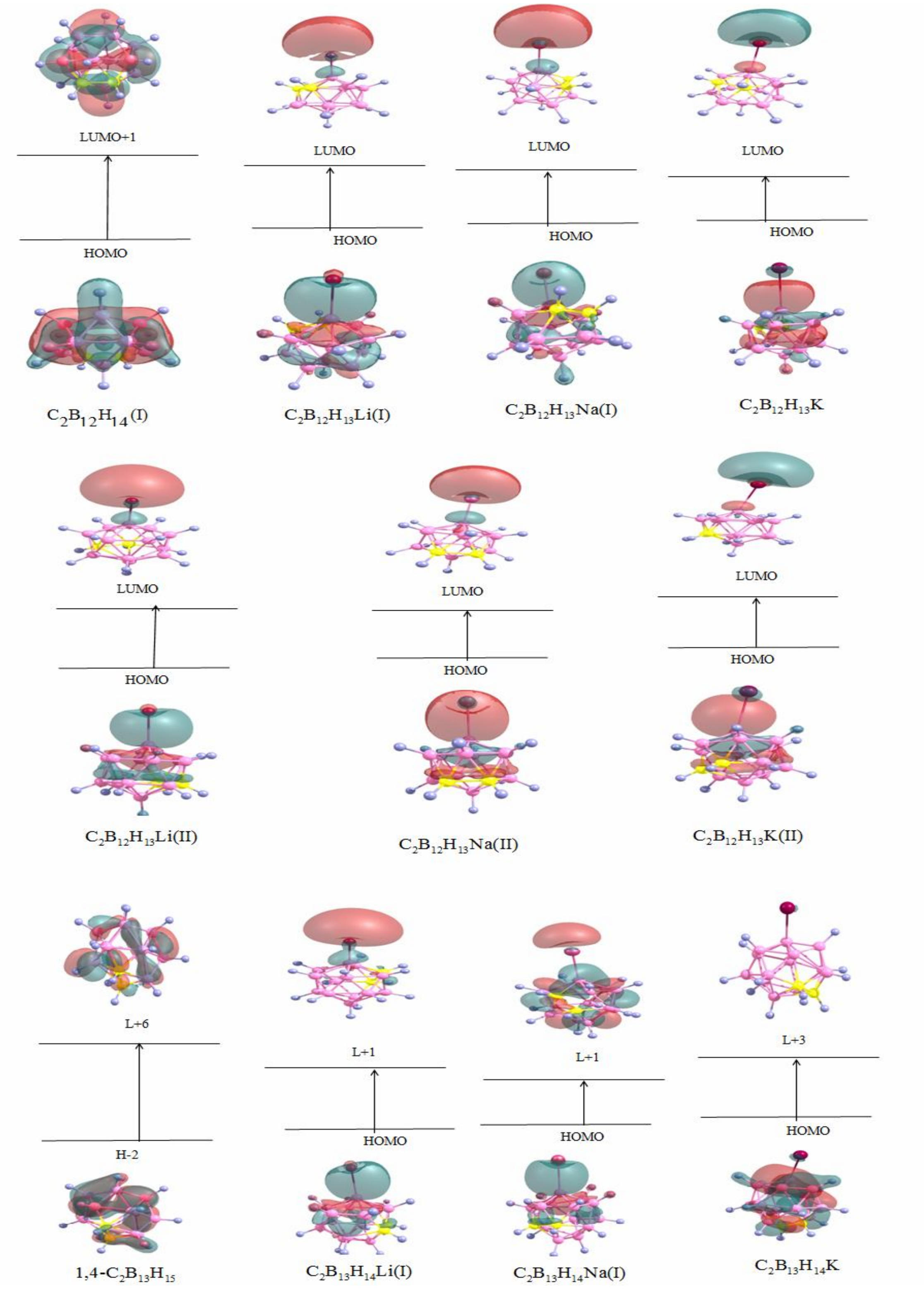

Fig. 3. The frontier molecular orbitals of alkali-metal substituted systems in their ground state and crucial excited state.

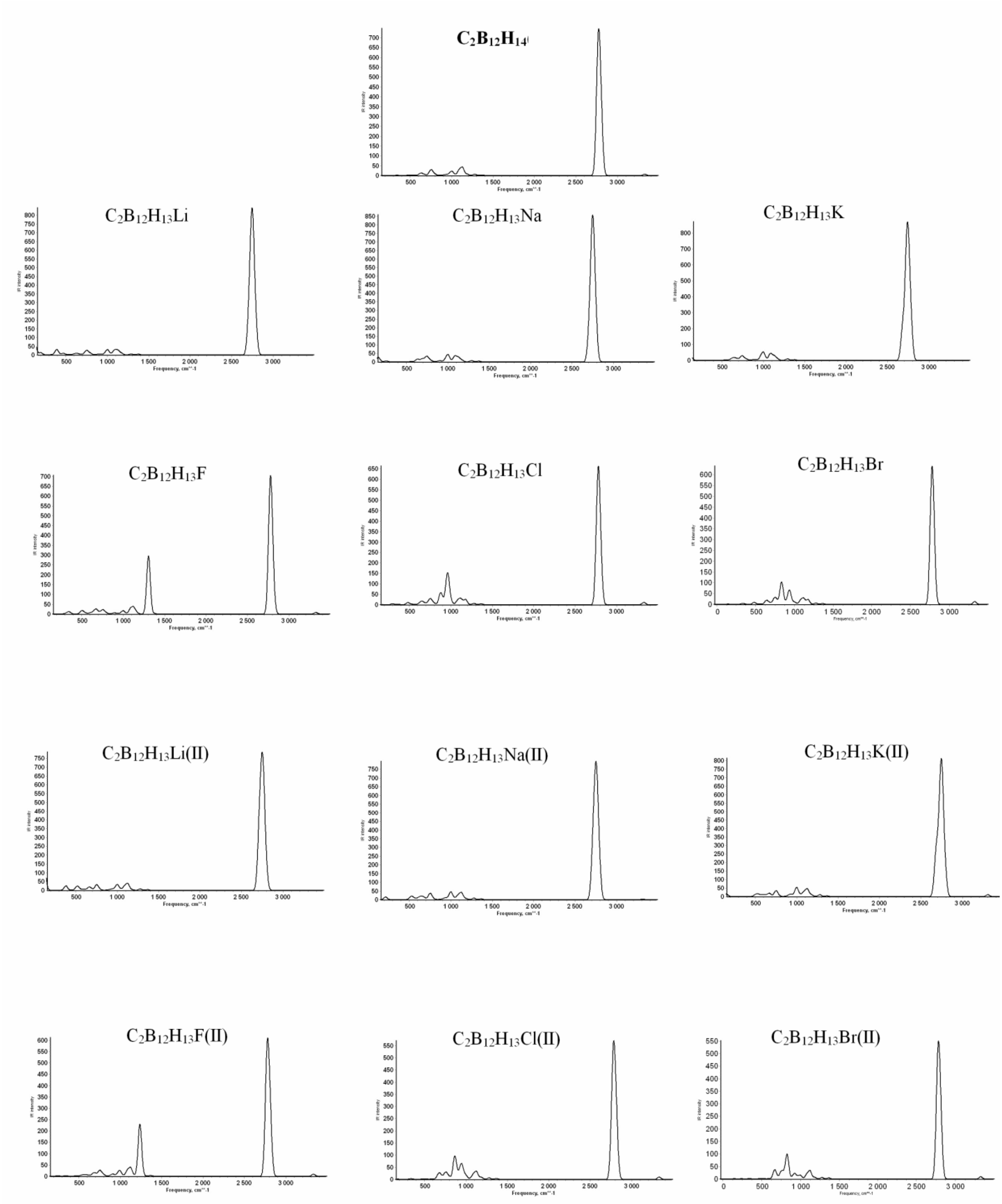

Fig. 4. The simulated vibrational spectrum of the studied structures.

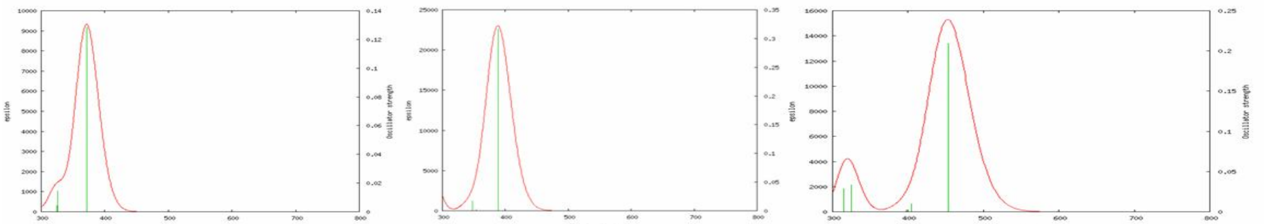

$C_2B_{12}H_{13}Li(I)$ $C_2B_{12}H_{13}Na(I)$ $C_2B_{12}H_{13}K(I)$

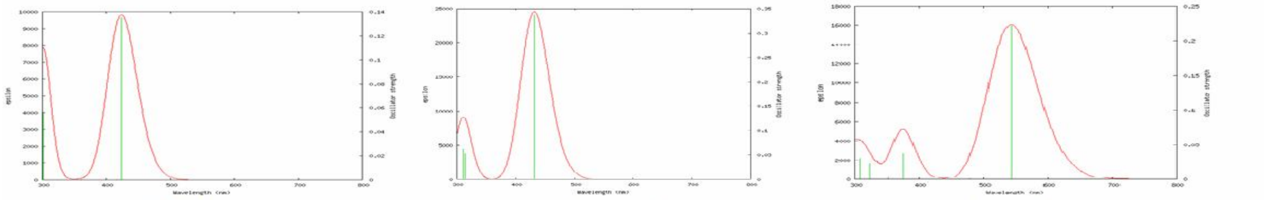

$C_2B_{12}H_{13}Li(II)$ $C_2B_{12}H_{13}Na(II)$ $C_2B_{12}H_{13}K(II)$

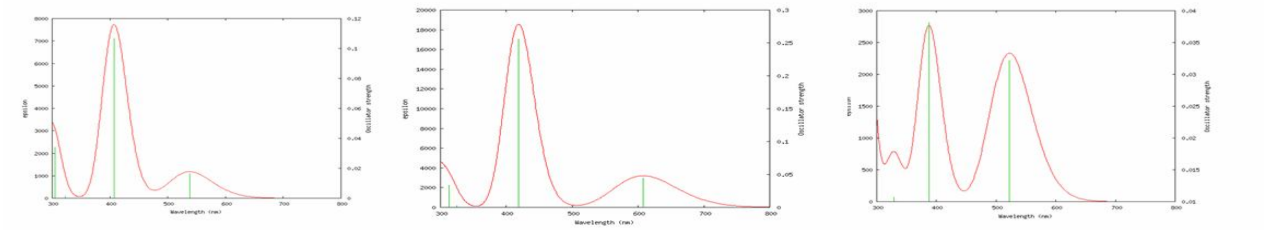

$C_2B_{13}H_{14}Li$ $C_2B_{13}H_{14}Na$ $C_2B_{13}H_{14}K$

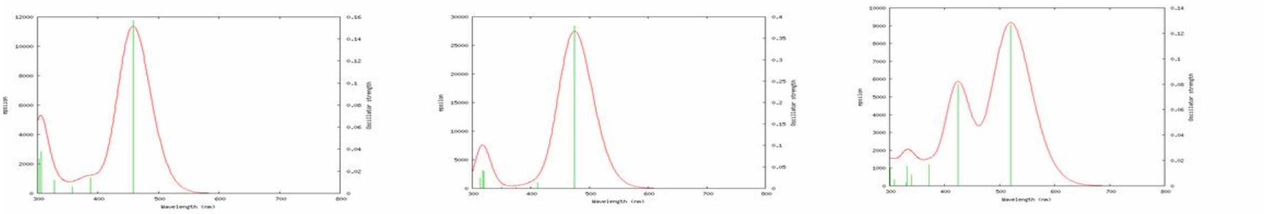

$C_2B_{14}H_{15}Li$ $C_2B_{14}H_{15}Na$ $C_2B_{14}H_{15}K$

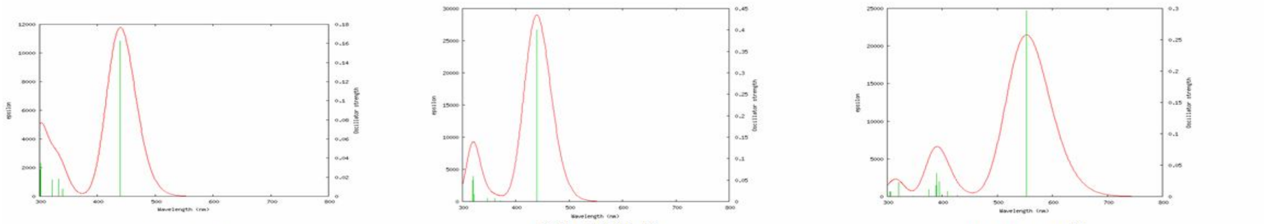

$C_2B_{15}H_{16}Li(I)$ $C_2B_{15}H_{16}Na(I)$ $C_2B_{15}H_{16}K(I)$

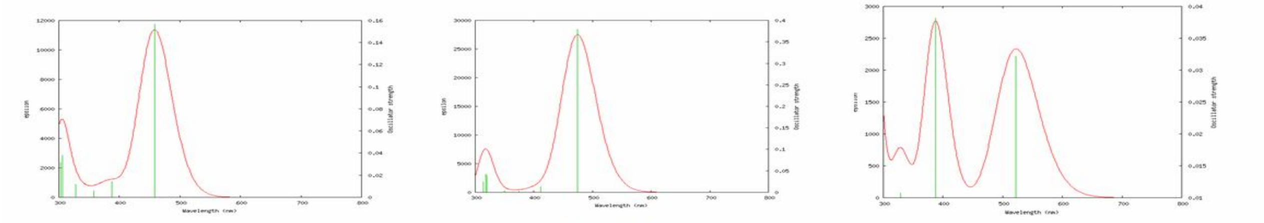

$C_2B_{15}H_{16}Li(II)$ $C_2B_{15}H_{16}Na(II)$ $C_2B_{15}H_{16}K(II)$

Fig. 5. Predicted electronic absorption spectrum of the of studied structures.

spectra of all these exhibit two or three main bands. The dual-band characteristic leads to the absorption broad.

CONCLUSIONS

In this study, the nonlinear optical properties of close-carborane derivatives are evaluated using DFT method. The results show that β_0 values for the substituted alkali metal carboranes are extremely large, while for the substituted halogen systems β_0 is vaguely enhanced. As a result, the alkali atoms cause a large β value. The large NLO response in substituted alkali metal carboranes is obtained by a lower transition energy, a larger oscillator strength, and a larger transition moment. Consequently, improvement in the NLO response is predicted for the considered carboranes produced by the alkali metals substitution, making them feasible systems for the design of nonlinear optical devices. The obtained results might provide a new insight for designing the novel NLO organometallic compounds.

REFERENCES

[1] Burland, D. M.; Miller, R. D.; Walsh, C. A., Second-order nonlinearity in poled-polymer systems. *Chem. Rev.* **1994**, *94*, 31-75, DOI: 10.1021/cr00025a002.

[2] Dalton, L. R.; Harper, A. W.; Ghosn, R.; Steier, W. H.; Ziari, M.; Fetterman, H.; Shi, Y.; Mustacich, R. V.; Jen, A. K. Y.; Shea, K. J., Synthesis and processing of improved organic second-order nonlinear optical materials for applications in photonics. *Chem. Mater.* **1995**, *7*, 1060-1081, DOI: 10.1021/cm00054a006.

[3] Marks, T. J.; Ratner, M. A., Design synthesis, and properties of molecule-based assemblies with large second-order optical nonlinearities. *Angew. Chem. Int. Ed. Engl.* **1995**, *34*, 155-173, DOI: 10.1002/anie.199501551.

[4] Bella, S. D.; Fragalà, I.; Ledoux, I.; Diaz-Garcia, M. A.; Marks, T. J., Synthesis haracterization, optical spectroscopic, electronic structure, and second-order nonlinear optical (NLO) properties of a novel class of donor-acceptor bis(salicylaldiminato)nickel(II) Schiff base NLO chromophores. *J. Am. Chem. Soc.* **1997**, *119*, 9550-9557, 10.1021/ja971349y.

[5] Nakano, M.; Fujita, H.; Takahata, M.; Yamaguchi, K., Theoretical study on second hyperpolarizabilities of phenylacetylene dendrimer: toward an understanding of structure-property relation in NLO responses of fractal antenna dendrimers. *J. Am. Chem. Soc.* **2002**, *124*, 9648-9655, DOI: 10.1021/ja0115969.

[6] Srinivas, K.; Sitha, S.; Jayathirtha Rao, V.; Bhanuprakash, K., Second-order nonlinear response in mono- and di-substituted triazine derivatives: a combined experimental and theoretical analysis. *Opt. Mater.* **2006**, *28*, 1006-1012, DOI: 10.1016/j.optmat.2005.05.011.

[7] Avramopoulos, A.; Reis, H.; Li, J.; Papadopoulos, M. G., The dipole moment, polarizabilities, and first hyperpolarizabilities of HArF: A computational and comparative study. *J. Am. Chem. Soc.* **2004**, *126*, 6179-6184, DOI: 10.1021/ja036319b.

[8] Coe, B. J.; Jones, L. A.; Harris, J. A.; Brunschwig, B. S.; Asselberghs, I.; Clays, K.; Persoons, A., Highly unusual effects of π-conjugation extension on the molecular linear and quadratic nonlinear optical properties of ruthenium(II) ammine complexes. *J. Am. Chem. Soc.* **2003**, *125*, 862-863, DOI: 10.1021/ja028897i.

[9] Plaquet, A.; Champagne, B.; Castet, F.; Ducasse, L.; Bogdan, E.; Rodriguez, V.; Pozzo, J. L., Theoretical investigation of the dynamic first hyperpolarizability of DHA-VHF molecular switches. *New J. Chem.* **2009**, *33*, 1349-1356, DOI: 10.1039/B900432G.

[10] Shakerzadeh, E.; Biglari, Z.; Tahmasebi, E., A quantum chemical study on the remarkable nonlinear optical and electronic characteristics of boron nitride nanoclusters by complexation *via* lithium atom. *J. Mol. Liquids.* **2016**, *221*, 443-451, DOI: 10.1016/j.molliq.2016.05.090.

[11] Kamalinahad, S.; Solimannejad, M.; Shakerzadeh, E., Nonlinear optical (NLO) response of pristine and functionalized dodecadehydrotribenzo annulene (DBA): A theoretical study. *Bull. Chem. Soc. J.* **2016**, *89*, 692-699, DOI: 10.1246/bcsj.20160006.

[12] Yousefizadeh, M.; Shakerzadeh, E.; Bamdad, M., Computational assessment of the electro-optical characteristics of the lithium doped boron clusters

LiBn (n = 4-11): A theoretical study. *Microelectronic Engineering* **2017**, *183*, 64-68, DOI: 10.1016/ j.mee.2017.10.011.

[13] Muhammad, S.; Xu, H.L.; Liao, Y.; Kan, Y. H.; Su, Z. M., Quantum mechanical design and structure of the Li@basket with a remarkably enhanced electro-optical response. *J. Am. Chem. Soc.* **2009**, *131*, 1183-1184, DOI: 10.1021/ja9032023.

[14] Chen, W.; Li, Z. R.; Wu, D.; Li, Y.; Sun, C. C.; Gu, F. L., The structure and the large nonlinear optical properties of Li@Calix [4] pyrrole. *J. Am. Chem. Soc.* **2005**, *127*, 10977-10981, DOI: 10.1021/ ja050601w.

[15] Hu, Y. Y.; Sun, S. L.; Muhammad, S.; Xu, H. L.; Su, Z. M., How the number and location of lithium atoms affect the first hyperpolarizability of graphene. *J. Phys. Chem. C* **2010**, *114*, 19792-19798, DOI: 10.1021/jp105045j.

[16] Wu, H. Q.; Zhong, R. L.; Sun, S. L.; Xu, H. L.; Su, Z. M., Alkali metals-substituted adamantanes lead to visible light absorption: large first hyperpolarizability. *J. Phys. Chem. C* **2014**, *118*, 6952-6958, DOI: 10.1021/jp410560j.

[17] Yousefizadeh, M.; Shakerzadeh, E.; Bamdad M., Electronic and nonlinear optical features of first row transition metals-decorated all-boron B40 fullerene: A promising route to remarkable electro-optical response. *Inorg. Chem. Commun.* **2020**, *112*, 107692, DOI: 10.1016/j.inoche.2019.107692.

[18] Li, X.; Jun, L., Giant enhancement of electronic polarizability and the first hyperpolarizability of fluoride-decorated graphene versus graphyne and graphdiyne: insights from ab initio calculations. *Phys. Chem. Chem. Phys.* **2019**, *21*, 13165-13175, DOI: 10.1039/C9CP01118H.

[19] Zhu, L.; Xue, K.; Hou, J., A theoretical study of alkaline-earthides $Li(NH_3)_4M$ (M = Be, Mg, Ca) with large first hyperpolarizability. *J. Mol. Model.* **2019**, *25*, 150, DOI: 10.1007/s00894-019-4042-3.

[20] Xu, H.; Li, Z.; Wu, D.; Wang, B.; Li, Y.; Gu, F.; Aoki, Y., Structures and large NLO responses of new electrides: Li-doped fluorocarbon chain. *J. Am. Chem. Soc.* **2007**, *129*, 2967-2970, DOI: 0.1021/ ja068038k.

[21] Endo, Y.; Ohta, K.; Yoshimi, O.; Yamaguchi, K., A new application of inorganic cluster, carboranes for medicinal drug design and molecular construction. *Phosphorus Sulfur Silicon Rel. Elements* **2004**, *179*, 799, DOI: 10.1080/10426500490427097.

[22] Schleyer, P. V. R.; Najafian, K., Stability and three-dimensional aromaticity of closo-monocarbaborane anions, and closo-Dicarboranes. *Inorg. Chem.* **1998**, *37*, 3454-3470, DOI: 10.1021/ic980110v.

[23] Lyubimov, S. E.; Rastorguev, E. A.; Verbitskaya, T. A.; Rastorguev, E. A.; Hey-Hawkins, E.; Kalinin, V. N.; Davankov, V. A., The use of a new carboranylamidophosphite ligand in the asymmetric Rh-catalyzed hydrogenation of α- and β-dehydroamino acid derivatives. *Polyhedron* **2011**, *30*, 1258-1261, DOI: 10.1016/j.poly.2011.02.003.

[24] Lyubimov, S. E.; Kuchurov, I. V.; Tyutyunov, A. A.; Petrovskii, P. V.; Kalinin, V. N.; Zlotin, S. G.; Davankov, V. A.; Hey-Hawkins, E., The use of new carboranylphosphite ligands in the asymmetric Rh-catalyzed hydrogenation. *Catalysis Commun.* **2010**, *11*, 419-421, DOI: 10.1016/j.catcom.2009.11.012.

[25] Lyubimov, S. E.; Davankov, V. A.; Gavrilov, K. N.; Grishina, T. B.; Rastorguev, E. A.; Tyutyunov A. A.; Verbitskaya, T. A.; Kalinin, V. N.; Hey-Hawkins, E., Diamidophosphites with isomeric carborane fragments: a comparison of catalytic activity in asymmetric Pd-catalyzed allylic substitution reactions. *Tetrahedron Lett.* **2010**, *51*, 1682-1684, DOI: 10.1016/j.tetlet.2010.01.084.

[26] Lyubimov, S. E.; Davankov, V. A.; Petrovskii, P. V.; Hey-Hawkins, E.; Tyutyunov, A. A.; Rys, E. G.; Kalinin, V. N., Chiral carborane-derived thiophosphites: A new generation of ligands for Rh-catalyzed asymmetric hydrogenation. *J. Organomet. Chem.* **2008**, *693*, 3689-3691, DOI: 10.1016/ j.jorganchem.2008.09.032.

[27] Keller, T. M., Oxidative protection of carbon fibers with poly(carborane-siloxane-acetylene). *Carbon* **2002**, *40*, 225-229, DOI: 10.1016/S0008-6223(01)00092-6.

[28] González-Campo, A.; Núñez, R.; Viñas, C.; Boury, B., Synthetic approaches to the preparation of hybrid network materials incorporating carborane clusters. *New J. Chem.* **2006**, *30*, 546-553, DOI: 10.1039/

B516705C.

[29] Valliant, J. F.; Guenther, K. J.; King, A. S.; Morel, P.; Schaffr, P.; Sogbein, O. O.; Stephenson, K. A., The medicinal chemistry of carboranes. *Coord. Chem. Rev.* **2002**, *232*, 173-230, DOI: 10.1016/S0010-8545(02)00087-5.

[30] Blanchard-Desce, M.; Alain, V.; Bedworth, P. V.; Marder, S. R.; Fort, A.; Runser, C.; Barzoukas, M.; Lebus, S.; Wortmann, R., Large quadratic hyperpolarizabilities with donor-acceptor polyenes exhibiting optimum bond length alternation: correlation between structure and hyperpolarizability. *Chem. Eur. J.* **1997**, *3*, 1091-1104, DOI: 10.1002/chem.19970030717.

[31] Shapiro, I.; Good, C.D.; Williams, R.E., The carborane series: BnC2Hn+2. I. $B_3C_2H_5$. *J. Am. Chem. Soc.* **1962**, *84*, 3837-3840, DOI: 10.1021/ja00879a010.

[32] Hawthorne, M. F.; Young, D. C.; Wegner, P. A., Carbametallic boron hydride derivatives. I. apparent analogs of ferrocene and ferricinium ion. *J. Am. Chem. Soc.* **1965**, *87*, 1818-1819, DOI: 10.1021/ja01086a053.

[33] Hosmane, N. S.; Maguire, J. A., Evolution of C_2B_4 carborane chemistry: from early years to the present. *Organometallics* **2005**, *24*, 1356-1389, DOI: 10.1021/om0490031.

[34] Krossing, I.; Raabe, I., Noncoordinating anions-fact or fiction? A survey of likely candidates. Angew. *Chem. Int. Ed.* **2004**, *43*, 2066-2090, DOI: 10.1002/anie.200300620.

[35] Hosmane, N. S.; Maguire, J. A., Recent advances in the chemistry of metallacarboranes. *Eur. J. Inorg. Chem.* **2003**, *22*, 3989-3999, DOI: 10.1002/ejic.200300259.

[36] Wedge, T. J.; Hawthorne, M. F., Multidentate carborane-containing Lewis acids and their chemistry: mercuracarborands. *Coord. Chem. Rev.* **2003**, *240*, 111-128, DOI: 10.1016/S0010-8545(02)00259-X.

[37] Xie, Z., Advances in the chemistry of metallacarboranes of f-block elements. *Coord. Chem. Rev.* **2002**, *231*, 23-46, DOI: 10.1016/S0010-8545(02)00112-1.

[38] Qudar, J. L.; Chemla, D. S., Hyperpolarizabilities of the nitroanilines and their relations to the excited state dipole moment. *J. Chem. Phys.* **1977**, *66*, 2664, DOI: 10.1063/1.434213.

[39] Weinhold, F.; Landis, C. R., Valency and bonding: a natural bond orbital donor-acceptor perspective. Cambridge University Press, 2005, p. 10-12.